A Compact Spherical RGBD Keyframe-based Representation

Tawsif Gokhool [1] , Renato Martins [1] , Patrick Rives [1] and Noëla Despré [2]
[1] Inria Sophia Antipolis, [2] Airbus Defense and Space

Introduction

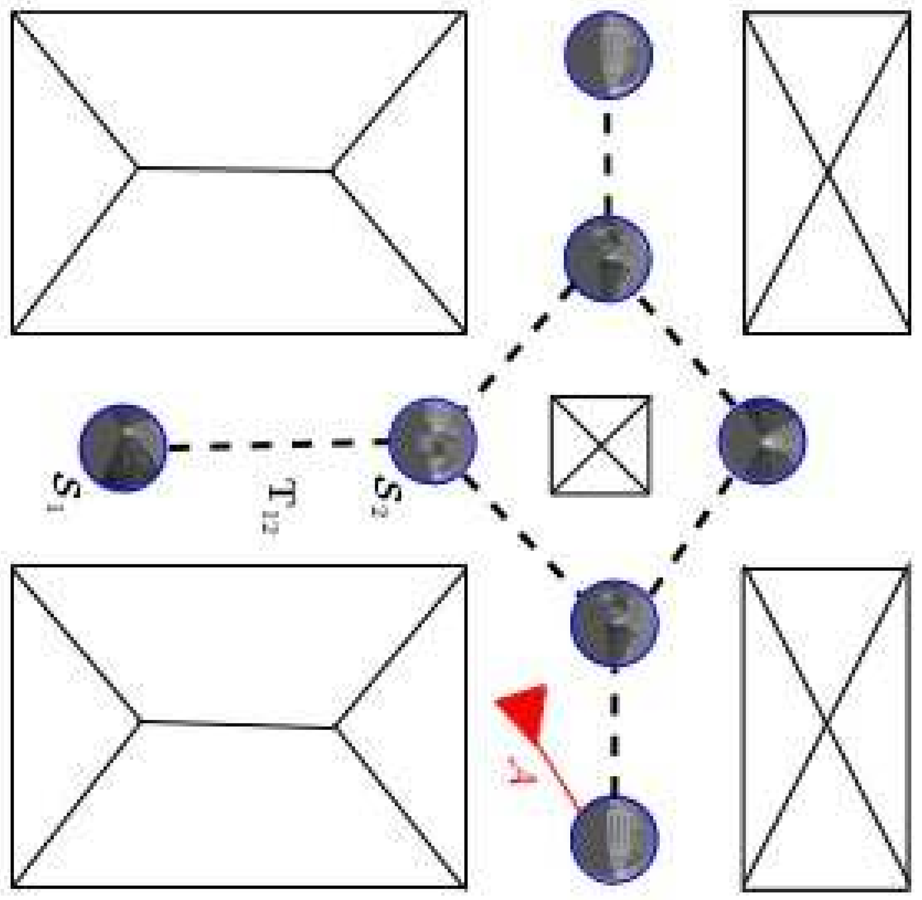

- Problem resolves around modelling of the environment using metric maps in a pose graph representation
- Relative motion of a mobile agent is computed using dense Spherical RGBD Visual Odometry (VO)

Spherical System Framework

Figure: Indoor sensor

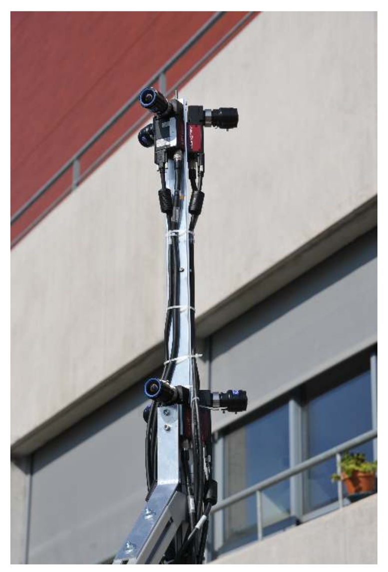

Figure: Outdoor sensor

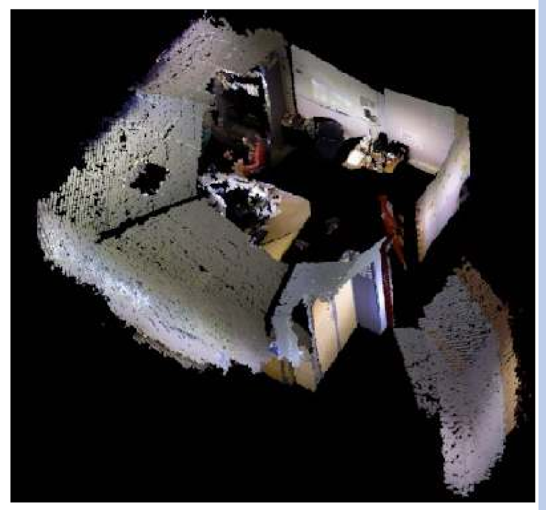

Figure: Point cloud representation

- Set of **augmented spheres** consist of both photometric and geometric information
- **360^0 FOV RGBD**
  - **Indoor**: image acquisition using Asus Xtion Pro live sensors
  - **Outdoor**: set of stereo cameras (depth from disparity)

Overall Approach Pipeline

Incremental pose and structure est. within **tree main stages**:

- warping $\mathcal{S}$ and its resulting model **error propagation**
- data **fusion** dealing with occlusions and outlier rejection
- **stable** salient points ranking

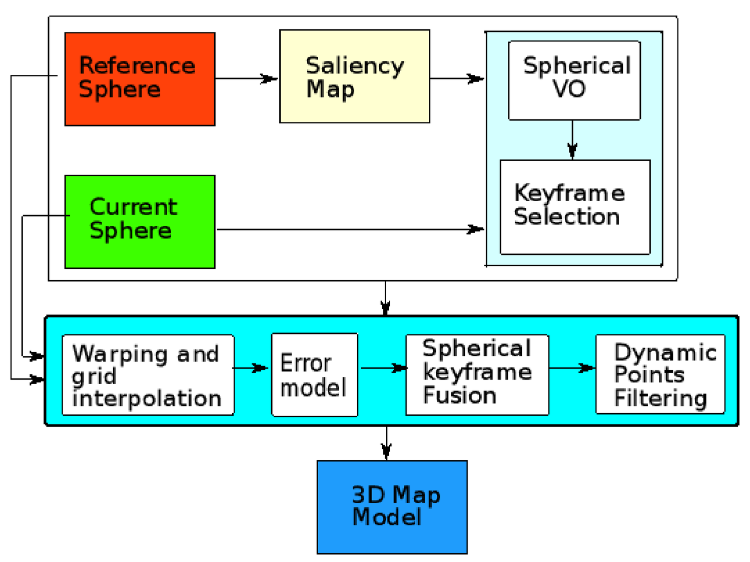

Uncertainty Modelling and Fusion

Propagating errors from structure and pose graph constraints:

$$\mathcal{D}_w(\mathbf{p}^*) = \mathcal{D}_t(w(\mathbf{p}^*, \mathbf{T})) \text{ and } \mathcal{D}_t(\mathbf{p}) = \sqrt{\mathbf{q}_w(\mathbf{p},\mathbf{T})^\top \mathbf{q}_w(\mathbf{p},\mathbf{T})}$$

$$\text{with } \mathbf{q}_w(\mathbf{p},\mathbf{T}) = \left([\mathbf{I}\ \mathbf{0}]\mathbf{T} \begin{bmatrix} g(\mathbf{p}) \\ 1 \end{bmatrix} \right)$$

$\mathcal{D}_t$:	warped depth		
$w(.)$:	warping function	$g(.)$:	inverse spherical projection
$\mathbf{q}_w$:	3D warped point	$\mathbf{T}$:	relative pose

- Registration using a *photo* + *geo* augmented cost function
- Chain of non-linear transformations of errors from the raw depth and pose $\mathbf{T}$
- Fuse the warped sphere and the keyframe model if contents are similar (entropy criteria)
- Outliers and occlusions handling following the decision rule:

$$\frac{(\mathcal{D}_w(\mathbf{p}) - \mathcal{D}^*(\mathbf{p}))^2}{\sigma^2_{\mathcal{D}_w}(\mathbf{p}) + \sigma^2_{\mathcal{D}^*}(\mathbf{p})} + \frac{(\mathcal{I}_w(\mathbf{p}) - \mathcal{I}^*(\mathbf{p}))^2}{\sigma^2_{I_w}(\mathbf{p}) + \sigma^2_{I^*}(\mathbf{p})} < \lambda^2_M,$$

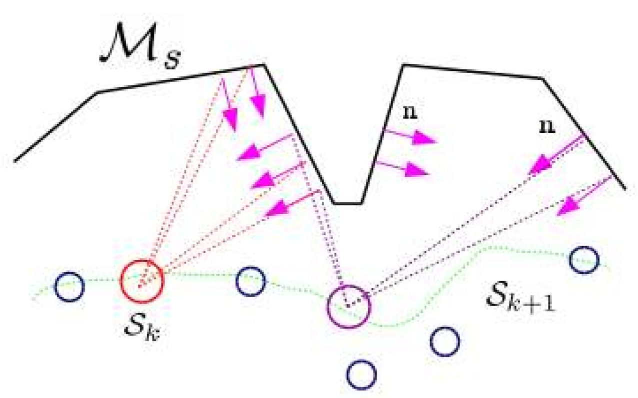

Figure: Scene errors and observability conditions

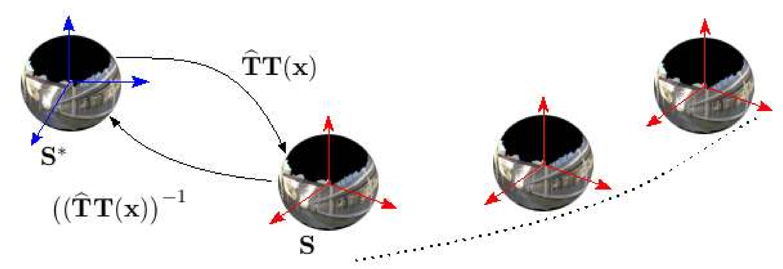

Figure: Registration and fusion

Stability Point Ranking and Saliency Criteria

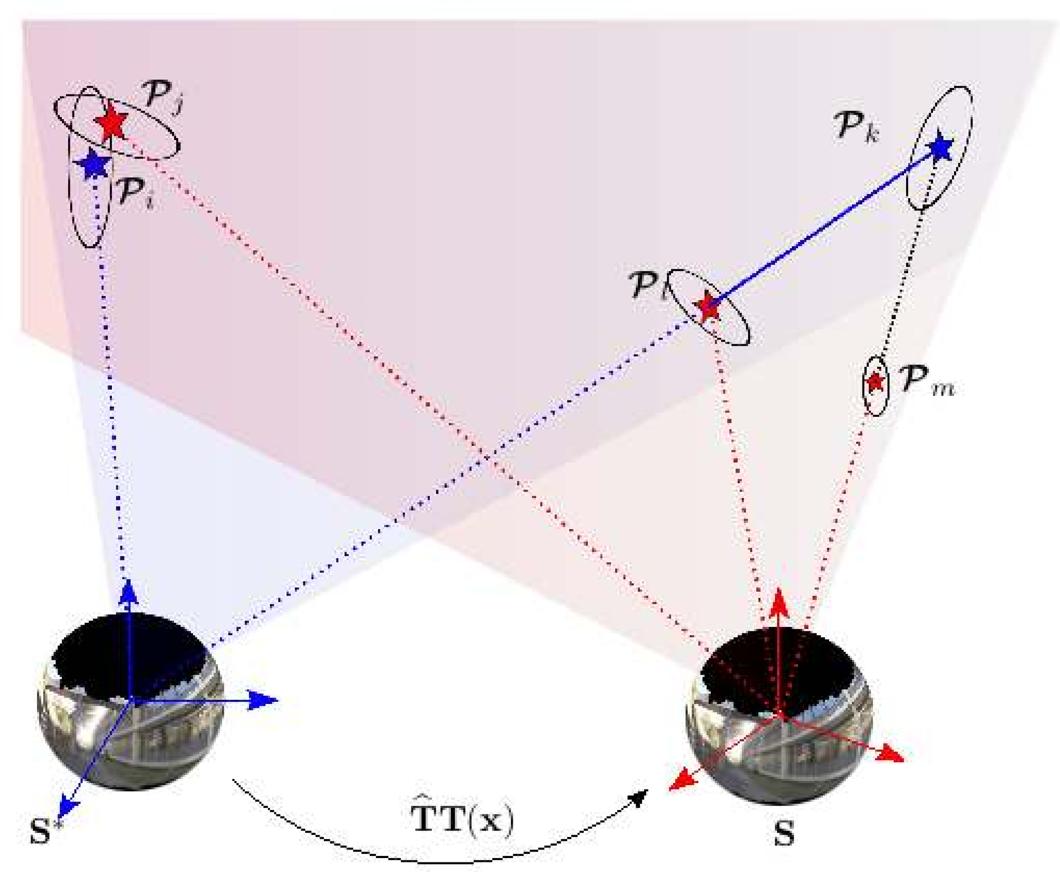

- Pixels observability from subsequent views
- Points perceived over several frames are made permanent
- Saliency map is used to label consistent features

Results: RGB-D Indoor and Outdoor Cases

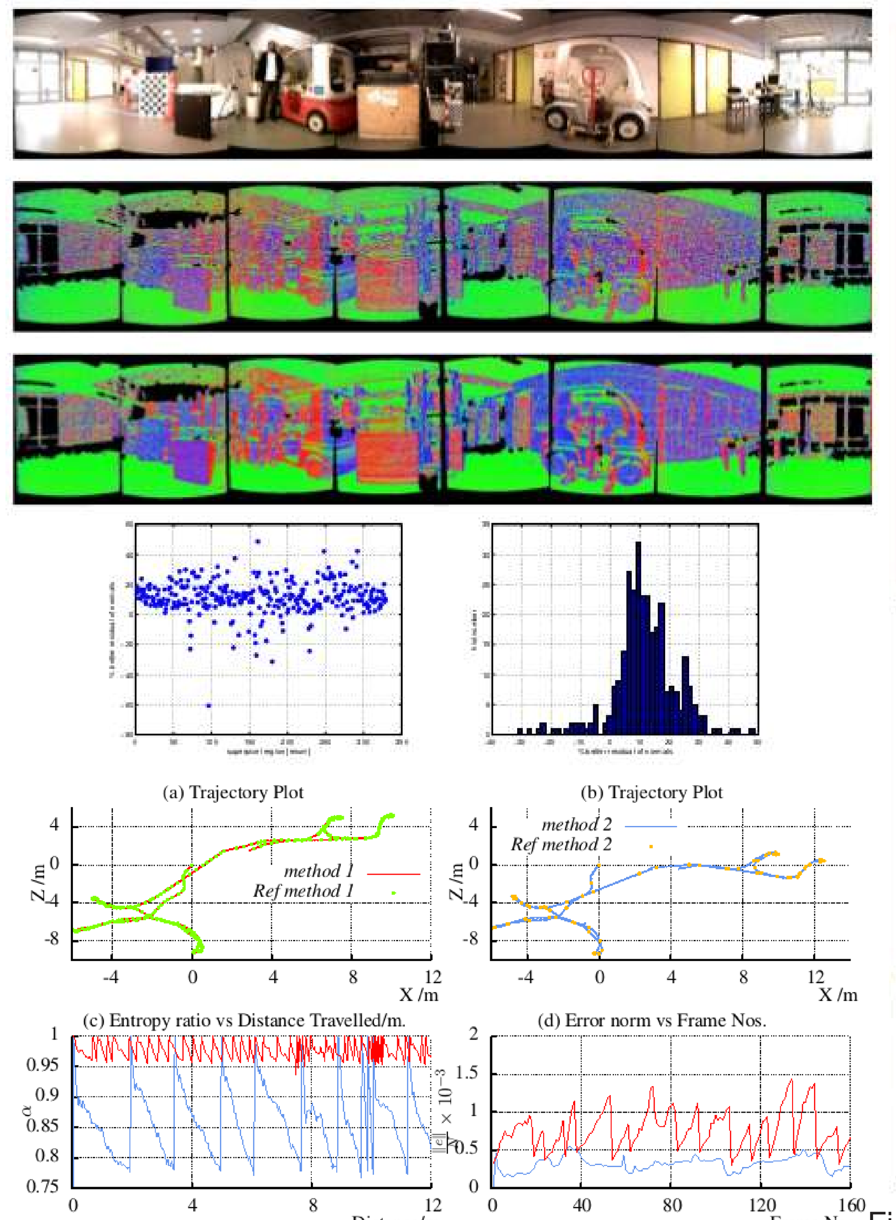

Figure: Comparison between laser and vision maps

- Normal's improvement of 20% in segmented planar patches
- 270 initially recorded keyframes are reduced to 67

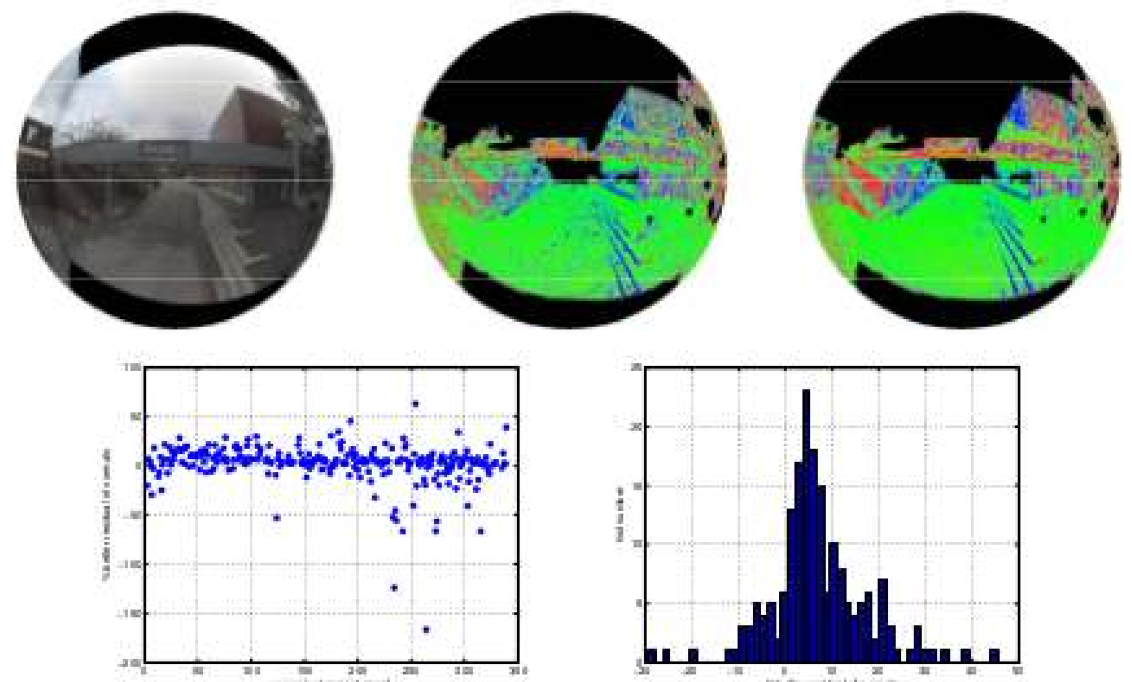

Figure: Normal surface consistency on raw sphere and filtered (top right) using 6 near spheres to the outdoor environment point-of-view showed (top left)

Conclusions

- Dense spherical RGB-D mapping approach
- **improvement** of 10% – 30% in the depth map
- **reduction** of keyframes, resulting in a sparser representation
- **better** overall consistency of the map
- **emergence** of two new entities: uncertainty and stability maps

Main References

- I. Dryanovski, R. Valenti, and J. Xiao. Fast visual odometry and mapping from RGB-D data. In *IEEE ICRA*, 2013.
- M. Meilland and A. Comport. On unifying keyframe and voxel based dense visual SLAM at large scales. In *IEEE IROS*, 2013.

Contact: renato-jose.martins@inria.fr